Solid−Liquid Phase Diagram for the System $MgCl_2-H_2O-C_2H_4(OH)_2$ at 333 K

Mark I. Pownceby,* David H. Jenkins, Roman Ruzbacky, and Sophia Saunders

CSIRO Process Science and Engineering, Bayview Avenue Clayton, Victoria 3168, Australia

This paper uses experimentally determined solid−liquid phase relation studies within the $MgCl_2-H_2O-C_2H_4(OH)_2$ ternary system to identify the origin of scale which formed in the packing of the dehydration column of the Australian Magnesium (AM) process for producing anhydrous magnesium chloride. The scale formed during dehydration of a purified magnesium chloride ($MgCl_2$) leach liquor plus recycled ethylene glycol ($C_2H_4(OH)_2$) solution. Experiments at 333 K showed the following phase fields present: a liquid-only phase region (Liq_T); three two-phase regions T + Liq_T, $MgCl_2 \cdot 6H_2O$ + Liqα, and $MgCl_2 \cdot 3[C_2H_4(OH)_2]$ + Liqβ; plus two three-phase regions $MgCl_2 \cdot 6H_2O$ + T + Liqα and $MgCl_2 \cdot 3[C_2H_4(OH)_2]$ + T + Liqβ. The compositions Liqα and Liqβ represent liquid compositions that extend a small distance into the ternary from the invariant points A and B located along the respective $MgCl_2-H_2O$ and $MgCl_2-C_2H_4(OH)_2$ binaries, while T represents a ternary phase of composition $MgCl_2 \cdot 2H_2O \cdot 2[C_2H_4(OH)_2]$. An additional four three-phase regions were predicted based on the existence of known crystalline phases. These included: $MgCl_2 \cdot 6H_2O$ + T + $MgCl_2 \cdot 4H_2O$, $MgCl_2 \cdot 4H_2O$ + T + $MgCl_2 \cdot 2H_2O$, $MgCl_2 \cdot 2H_2O$ + T + $MgCl_2$, and $MgCl_2$ + T + $MgCl_2 \cdot 3[C_2H_4(OH)_2]$. The ternary compound was identified as the solid that precipitated within the dehydration column. Additional testwork between (293 and 363) K indicated that the position of the solid−liquid boundary was relatively insensitive to temperature changes.

Introduction

This paper describes the results of experiments conducted at 333 K to determine solid−liquid phase relations in the $MgCl_2-H_2O-C_2H_4(OH)_2$ ternary system.

Between 1993 and 1994, the Australian Magnesium Corporation (AMC) built a batch minipilot plant and a continuous minipilot plant (CMPP) to test the unit operations of the Australian Magnesium (AM) process. This was followed by the design and construction of a 1500 tpa Demonstration Plant at Gladstone in Queensland, Australia, to produce magnesium metal.[1]

At the front end of the AM process, purified magnesium chloride leach liquor ($MgCl_2$) plus recycled ethylene glycol ($C_2H_4(OH)_2$) solution are added to a train of dehydration columns (Figure 1). The ethylene glycol replaces the water as solvent for the magnesium chloride solute for recovery of an essentially water-free $MgCl_2-C_2H_4(OH)_2$ solution.[1]

During operation of the CMPP, a precipitate was observed to form on the packing below the feed point of the No. 1 dehydration column. The precipitate gradually blocked the packing, which resulted in a large column pressure drop and eventual column flooding. After four episodes of blocking, the No. 1 column on the CMPP was bottom-fed to prevent continued scaling of the packing.

As a consequence of the top-feeding problems on the CMPP, bottom-feeding of the No. 1 dehydration column was initially implemented on the Demonstration Plant. However, while a satisfactory level of dehydration was obtained producing $MgCl_2-C_2H_4(OH)_2$ solutions containing ~400 ppm H_2O, bottom-feeding translated into a significant energy penalty. During distillation, the column packing needs to be continually wet to achieve efficient mass transfer between the gas and liquid phases. This was achieved by the addition of distillate reflux water at the top of the column, but the extra water also needs to be removed, representing an additional energy cost. In comparison, top-feeding of the column does not require additional reflux water to wet the packing, resulting in a significant reduction in operating costs. Top-feeding of the column was therefore the preferred option by AMC provided the problems of scale formation at the feed point can be overcome.

Examination of the precipitate by optical microscopy and X-ray diffraction showed the scale that formed during top-feeding consisted of a white, amorphous material. Chemical analysis indicated that it contained Mg, Cl, $C_2H_4(OH)_2$, and H_2O, the major components of the feed solution. If phase relations within the simple $MgCl_2-H_2O-C_2H_4(OH)_2$ ternary system could be determined, then the composition and stability range of scale formation may be understood, and removal or avoidance strategies during column top-feeding could be implemented.

A temperature of 333 K was initially used for the solid−liquid phase experiments as this represented conditions near the top of the dehydration column where scale formation was known to occur. In addition, preliminary experiments were conducted within the temperature range (293 to 363) K to examine the influence of temperature on the position of phase boundaries, in particular, the position of the solid−liquid phase boundary.

Experimental Section

Reagents. The anhydrous magnesium chloride was BDH laboratory reagent grade comprising > 99.7 % $MgCl_2$ and 0.3 % adsorbed water. Ethylene glycol was Chem-Supply Technical grade ethylene glycol (98 % minimum) with a measured water content of < 0.03 %. The magnesium chloride hexahydrate ($MgCl_2 \cdot 6H_2O$) used was BDH analytical reagent grade with a magnesium content of 46.7 % (by weight) and a molar ratio for $MgCl_2$:H_2O of 1:6.03.

* Corresponding author. E-mail: mark.pownceby@csiro.au.

10.1021/je100293k Published 2010 by the American Chemical Society
Published on Web 07/07/2010

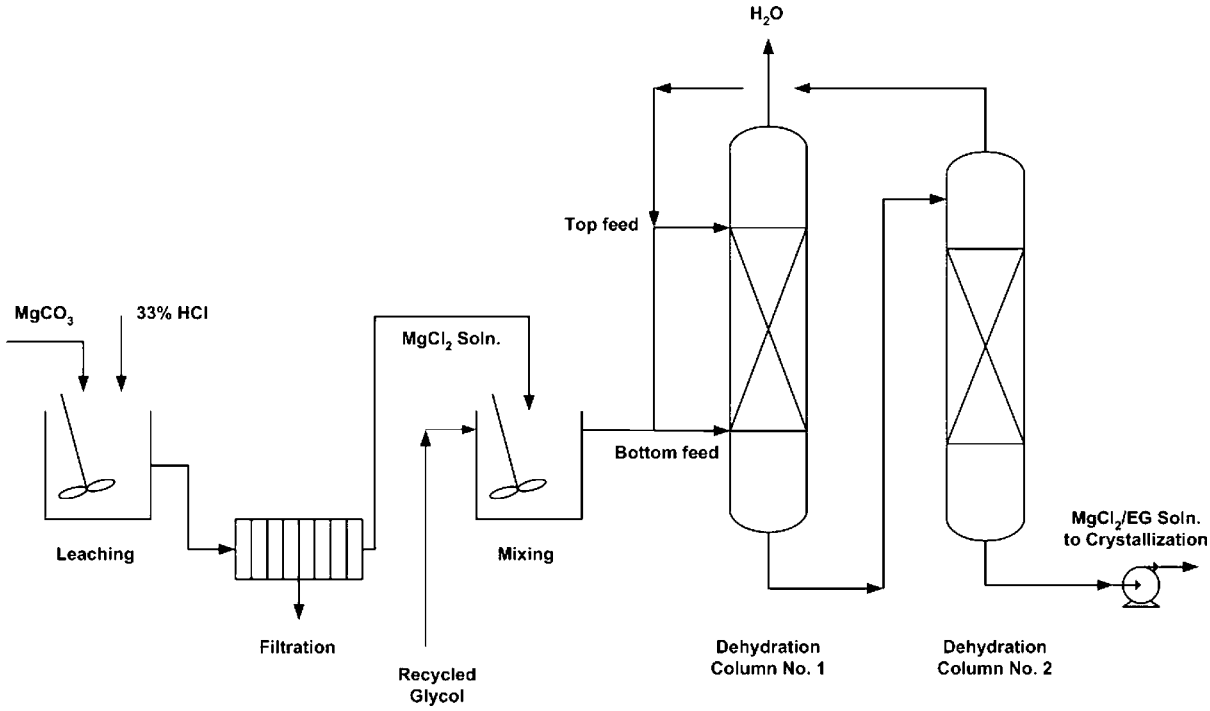

Figure 1. Schematic diagram of the front end of the AM process. EG refers to ethylene glycol (after Jenkins et al.[1]).

Analytical Procedures. Water. The water content in the solid phases and liquors was determined using a Metrohm 701 Karl Fischer (KF) Titrino apparatus using a stable hydranal hydrazine solution of iodine, sulfur dioxide, and imidazole dissolved in alcohol. All titrations were carried out in duplicate and gave a consistent relative standard deviation (2σ) of $\pm$ 2 %.

Magnesium, Chlorine, and Ethylene Glycol. At the completion of all experiments, the recovered liquid and solid phases were dissolved in 10 mL of 10 % nitric acid and made up to 100 mL of total volume with distilled and deionized water. Magnesium was determined by titration with a standard 0.1 M ethylenediaminetetraacetic acid (EDTA) solution, while chloride was measured potentiometrically using a Metrohm 672 Titroprocessor. For all compositions, ethylene glycol was determined by difference.

X-ray Diffraction. X-ray diffraction (XRD) was used to characterize the solid phases. Samples were filtered using a Millipore filter to recover the solid phase, which was then dried to constant weight in an oven at 333 K before being loaded in an aluminum sample holder for X-ray diffraction analysis.

X-ray diffraction patterns were collected using a Phillips PW1710 powder diffractometer fitted with a diffracted beam graphite monochromator and employing Cu Kα radiation. The diffractometer was operated at 40 keV and 40 mA, and samples were analyzed over the range 5° to 65° 2θ using a step size of 0.04° 2θ and counting times of 0.25 s per step. Total scan times were of the order of (10 to 12) min per sample.

In experiments in which the triglycollate phase $MgCl_2 \cdot 3[C_2H_4(OH)_2]$ formed part of the equilibrium assemblage (see below), the solid sample was X-rayed wet by smearing the slurry onto the holder. Preliminary testwork, however, showed that exposure of $MgCl_2 \cdot 3[C_2H_4(OH)_2]$ to a moist atmosphere, even for a brief time, resulted in conversion to an amorphous, hydrated phase that could not be identified by XRD analysis. To avoid reaction with water vapor in the atmosphere, the wet slurry sample was covered with a clear plastic film of low density polyethylene before analysis.

Methods. Solid−Liquid Equilibration Experiments. Solid−liquid equilibration experiments were initially performed along the $MgCl_2-C_2H_4(OH)_2$ and $MgCl_2-H_2O$ binaries to determine (a) the maximum solubility (saturation) of $MgCl_2$ in ethylene glycol and water and (b) the composition of any solid binary compounds at saturation.

In each experiment, excess $MgCl_2$ was added to the solvent in a 250 mL Schott bottle. The temperature of reaction was kept constant at (333 $\pm$ 5) K by partially immersing the reaction vessel in an agitated glycol bath. In preliminary experiments the reaction times varied between (24 and 48) h, with an additional settling time of 24 h to effect separation between solid and liquid phases. Results for both systems indicated that equilibrium was reached after 48 h (plus the 24 h settling time for solids). Thereafter, all experiments employed a regime of 48 h reaction time (with agitation) followed by 24 h settling time.

Experiments to determine solid−liquid phase relations within the ternary $MgCl_2-H_2O-C_2H_4(OH)_2$ system used weighed amounts of solid and liquid reactants also prepared in sealed 250 mL Schott bottles. These were also agitated for 48 h in a glycol bath at (333 $\pm$ 5) K, followed by a 24 h settling time for separation of the solid phases.

Effect of Temperature Experiments. In experiments to examine the effect of temperature on the phase relations, components were added to 500 mL round-bottom flasks equipped with a three-bladed glass propeller agitator, thermowell, feed port, and vent. The reaction flask was kept at constant temperature via a heating mantle, and an overhead stirrer was used to mix the contents at a constant rate of 420 rpm. A thermocouple was placed inside the thermowell for temperature read-out, and the temperature was gradually decreased in 10 K intervals from 363 K down to 333 K. Solutions were kept at each temperature for ~10 min stirring time followed by ~15 min settling time.

Results and Discussion

$MgCl_2-H_2O$ Binary. Solid hydrate phases stable at 333 K along the $MgCl_2-H_2O$ binary include the dihydrate ($MgCl_2 \cdot 2H_2O$), the tetrahydrate ($MgCl_2 \cdot 4H_2O$), and the hexahydrate ($MgCl_2 \cdot 6H_2O$). The hexahydrate and tetrahydrate have incongruent melting points at (390.3 and 454) K, respectively.[2] The dihydrate crystallizes from $MgCl_2$ solutions above 454 K; however, reliable solubility data are not available.

At 333 K, the maximum solubility of $MgCl_2$ along the $MgCl_2-H_2O$ binary join is reported to be 37.9 %.[3] Results from this study confirmed the maximum solubility at 333 K to be 37.9 % (by weight) based on an average of three replicate runs. The stable crystalline phase in equilibrium with the $MgCl_2$ saturated liquid was $MgCl_2 \cdot 6H_2O$.

$MgCl_2-C_2H_4(OH)_2$ Binary. The only stable phase reported to occur along the $MgCl_2-C_2H_4(OH)_2$ binary is the magnesium chloride triglycollate phase, $MgCl_2 \cdot 3[C_2H_4(OH)_2]$.[4-6] The solubility of $MgCl_2$ in ethylene glycol at 333 K was measured at 12.2 % (by weight) based on an average of three replicate runs. The stable crystalline phase in equilibrium with the $MgCl_2$ saturated liquid was $MgCl_2 \cdot 3[C_2H_4(OH)_2]$.

$MgCl_2-H_2O-C_2H_4(OH)_2$ Ternary. Thirty-one compositions were prepared to locate the positions of phase boundaries within the $MgCl_2-H_2O-C_2H_4(OH)_2$ ternary. Initial starting compositions, resulting phase assemblages, and assays for all liquid phases are given in Table 1.

X-ray diffraction indicated that the solid phases present in the $MgCl_2-H_2O-C_2H_4(OH)_2$ system were: $MgCl_2 \cdot 6H_2O$, $MgCl_2 \cdot 3[C_2H_4(OH)_2]$, and a previously unknown white, wax-like sludge material, hereafter denoted T-phase. Representative XRD patterns for these phases are shown in Figure 2. Note that it was not possible to obtain a unique X-ray pattern for $MgCl_2 \cdot 3[C_2H_4(OH)_2]$ as exposure of this compound to a moist atmosphere resulted in conversion to an amorphous hydrated phase. Samples in which the triglycollate was present produced X-ray patterns that had reduced intensities and a characteristic broad hump between ~15° and 35° 2θ (e.g., patterns (d) and (e) in Figure 2).

To identify the composition of the T-phase, the solid from bulk compositions in which the assemblage T-phase + Liq formed was recovered by filtering, drying at 333 K, and then assaying. Chemical analysis gave a composition containing 37.2 % $MgCl_2$, 14.2 % H_2O, and 48.6 % ethylene glycol by difference (all in % by weight), which indicated that the chemical composition of the T-phase was $MgCl_2 \cdot 2H_2O \cdot 2[C_2H_4(OH)_2]$, the ideal composition of which is: 37.3 % $MgCl_2$, 14.1 % H_2O, and 48.6 % ethylene glycol.

Low voltage SEM images of dried T-phase crystals showed that the T-phase formed characteristically small, well-formed hexagonal shaped crystals (Figure 3a). In comparison, examination of the dried solid recovered from compositions where the T-phase crystallized with magnesium chloride triglycollate (e.g., runs MWE 41, 43, and 44) suggested that the T-phase may also exhibit a long, needle-shaped crystal habit. For example, when X-rayed moist, run MWE 43 contained both T-phase and $MgCl_2 \cdot 3[C_2H_4(OH)_2]$ as the primary crystalline assemblage but after drying, the X-ray pattern showed only the T-phase to be present. SEM examination of the dried solid (Figure 3b) clearly showed two different phase morphologies: the typical small, euhedral T-phase crystal habit plus a second, long, needle-like crystalline phase. The disappearance of the triglycollate phase after drying and subsequent exposure to air suggested that the magnesium triglycollate reacted with moisture in the atmosphere forming the T-phase plus free glycol. The newly formed T-phase retained the crystal morphology of the original magnesium triglycollate crystals indicating the hydration reaction is a pseudomorphic replacement process.

The experimental results in Table 1 have been plotted on a ternary phase diagram in Figure 4. On the basis of these data, the $MgCl_2-H_2O-C_2H_4(OH)_2$ system at 333 K consists of at least six separate phase regions. These are:

(1) A ternary, liquid-only phase region (Liq_T) containing $MgCl_2$, H_2O, and ethylene glycol components in solution. The liquid composition within the phase region is dominated by high H_2O and ethylene glycol contents and extends from the invariant $MgCl_2$ saturation composition along the $MgCl_2-H_2O$ binary (point A in Figure 4) to the invariant $MgCl_2$ saturation composition along the $MgCl_2-C_2H_4(OH)_2$ binary (point B).

(2) A two-phase region containing the assemblage T + Liq_T. For any bulk composition within this region, the T-phase coexists with a ternary liquid composition which lies along the solid−liquid boundary extending between points A and B on the binaries.

(3) The two-phase regions $MgCl_2 \cdot 6H_2O$ + Liqα and $MgCl_2 \cdot 3[C_2H_4(OH)_2]$ + Liqβ where Liqα and Liqβ represent small, finite extensions from points A and B into the ternary.

(4) Two three-phase regions characterized by the assemblages $MgCl_2 \cdot 6H_2O$ + T + Liqα and $MgCl_2 \cdot 3[C_2H_4(OH)_2]$ + T + Liqβ.

The extension from points A and B into the ternary and leading to the formation of the $MgCl_2 \cdot 6H_2O$ + Liqα and $MgCl_2 \cdot 3[C_2H_4(OH)_2]$ + Liqβ phase fields was verified by the observation that in experiments containing the assemblage $MgCl_2 \cdot 6H_2O$, T-phase, and liquid the liquid compositions contained up to (4 to)5 % (by weight) ethylene glycol (i.e., they did not produce a liquid with the ethylene glycol-free composition corresponding to point A along the $MgCl_2-H_2O$ binary). Similarly, in experiments producing the assemblage $MgCl_2 \cdot 3[C_2H_4(OH)_2]$, T-phase, and liquid, the liquid compositions consistently recorded elevated water levels (Table 1). For example, water contents in the liquid coexisting with $MgCl_2 \cdot 3[C_2H_4(OH)_2]$ along the $MgCl_2-C_2H_4(OH)_2$ binary (i.e., point B) contained a maximum of ~0.25 % (by weight) water, whereas in the phase region where the assemblage $MgCl_2 \cdot 3[C_2H_4(OH)_2]$, T-phase, and liquid was stabilized the water contents in the liquid were ~2 % (by weight). The 0.25 % (by weight) water along the water-absent binary indicates the amount of water resulting from exposure (contamination) by the atmosphere; however, an increase to ~2 % (by weight) in the presence of the T-phase suggests partial solubility of water in the originally water-free liquid according to the equilibria

$$MgCl_2 \cdot 3[C_2H_4(OH)_2]\,(s) + 2H_2O\,(l) = MgCl_2 \cdot 2H_2O \cdot 2[C_2H_4(OH)_2]\,(s) + 2C_2H_4(OH)_2\,(l) \quad (1)$$

In the same way, the (4 to 5) % (by weight) ethylene glycol measured in the liquid when $MgCl_2 \cdot 6H_2O$ coexists with the T-phase indicates partial solubility of ethylene glycol according to

$$MgCl_2 \cdot 6H_2O\,(s) + 2C_2H_4(OH)_2\,(l) = MgCl_2 \cdot 2H_2O \cdot 2[C_2H_4(OH)_2]\,(s) + 2H_2O\,(l) \quad (2)$$

As well as the phase regions described above, there is likely to be an additional four phase regions based on the surrounding phase topology and the known stability of the dihydrate ($MgCl_2 \cdot 2H_2O$) and tetrahydrate ($MgCl_2 \cdot 4H_2O$) phases. The projected phase regions include: $MgCl_2 \cdot 6H_2O$ + T + $MgCl_2 \cdot 4H_2O$, $MgCl_2 \cdot 4H_2O$ + T + $MgCl_2 \cdot 2H_2O$, $MgCl_2$ + T + $MgCl_2 \cdot 3[C_2H_4(OH)_2]$, and $MgCl_2 \cdot 2H_2O$ + T + $MgCl_2$.

Table 1. Starting Compositions and Experimental Conditions from Experiments in the $MgCl_2-H_2O-C_2H_4(OH)_2$ Ternary at 333 K

.	bulk composition (%)				liquid assay (%)		
run no.	$MgCl_2$	H_2O	EG[a]	assemblage	$MgCl_2$	H_2O	EG[a]
MWE 1A	23.42	71.00	5.58	liquid only	24.00	69.07	6.93
MWE 1B				liquid only	23.87	69.12	7.01
MWE 2A	20.83	68.06	11.11	liquid only	21.16	65.84	13.00
MWE 2B				liquid only	21.62	65.55	12.83
MWE 3A	18.23	65.10	16.67	liquid only	18.97	63.95	17.08
MWE 3B				liquid only	18.63	63.28	18.09
MWE 4A	32.46	59.85	7.69	liquid only	32.83	55.49	11.68
MWE 4B				liquid only	33.00	55.71	11.29
MWE 5A	28.85	55.77	15.38	liquid only	29.14	54.37	16.49
MWE 5B				liquid only	28.96	54.36	16.68
MWE 6A	25.25	51.67	23.08	liquid only	25.74	51.12	23.14
MWE 6B				liquid only	25.43	50.67	23.90
MWE 7A	18.75	21.25	60.00	T-phase + liquid	15.68	22.40	61.92
MWE 7B				T-phase + liquid	16.02	22.43	61.55
MWE 8A	14.06	15.94	70.00	T-phase + liquid	13.83	15.60	70.57
MWE 8B				T-phase + liquid	13.55	16.39	70.06
MWE 9A	9.38	10.62	80.00	liquid only	10.08	10.04	79.88
MWE 9B				liquid only	9.94	10.07	79.99
MWE 13A	23.44	26.56	50.00	T-phase + liquid	17.60	29.86	52.54
MWE 13B				T-phase + liquid	17.83	30.51	51.66
MWE 14A	20.00	30.00	50.00	T-phase + liquid	19.16	32.26	48.58
MWE 14B				T-phase + liquid	18.80	32.04	49.16
MWE 15A	25.00	35.00	40.00	T-phase + liquid	22.40	40.87	36.73
MWE 15B				T-phase + liquid	23.31	40.85	35.84
MWE 16AL	15.63	34.37	50.00	liquid only	16.68	34.88	48.44
MWE 16BL				liquid only	16.75	34.97	48.28
MWE 17AL	12.50	27.50	60.00	liquid only	13.29	28.02	58.69
MWE 17BL				liquid only	13.19	27.92	58.89
MWE 18AL	10.16	19.84	70.00	liquid only	11.13	21.01	67.86
MWE 18BL				liquid only	10.88	20.68	68.44
MWE 19A	20.00	40.00	40.00	liquid only	21.09	40.51	38.40
MWE 19B				liquid only	21.66	40.57	37.77
MWE 20A	25.00	45.00	30.00	T-phase + liquid	25.93	47.29	26.78
MWE 20B				T-phase + liquid	26.38	46.98	26.64
MWE 21A	30.00	48.00	22.00	T-phase + liquid	31.38	54.61	14.01
MWE 21B				T-phase + liquid	31.31	53.66	15.03
MWE 22AL	32.00	53.00	15.00	T-phase + liquid	34.12	55.13	10.75
MWE 22BL				T-phase + liquid	33.09	54.19	12.72
MWE 23AL	38.00	57.00	5.00	$MgCl_2 \cdot 6H_2O$ + T-phase + Liqα	38.85	56.74	4.41
MWE 23BL				$MgCl_2 \cdot 6H_2O$ + T-phase + Liqα	37.66	57.01	5.33
MWE 26A	16.00	10.00	74.00	T-phase + liquid	14.38	9.95	75.67
MWE 26B				T-phase + liquid	13.90	10.12	75.98
MWE 28A	12.60	0.00	87.40	[b]$MgCl_2 \cdot 3EG$ + Liqβ	13.03	0.25	86.72
MWE 28B				$MgCl_2 \cdot 3EG$ + Liqβ	12.99	0.25	86.76
MWE 30A	15.00	5.25	79.75	T-phase + liquid	12.42	5.71	81.87
MWE 30B				T-phase + liquid	11.97	6.04	81.99
MWE 32A	12.61	0.00	87.39	$MgCl_2 \cdot 3EG$ + Liqβ	12.01	0.25	87.74
MWE 32B				$MgCl_2 \cdot 3EG$ + Liqβ	12.22	0.25	87.53
MWE 33A	24.70	42.60	32.70	T-phase + liquid	25.25	44.25	30.50
MWE 33B				T-phase + liquid	25.43	44.50	30.07
MWE 35A	36.00	54.00	10.00	$MgCl_2 \cdot 6H_2O$ + T-phase + Liqα	38.19	57.38	4.43
MWE 35B				$MgCl_2 \cdot 6H_2O$ + T-phase + Liqα	38.70	57.70	3.60
MWE 37A	38.50	59.00	2.50	$MgCl_2 \cdot 6H_2O$ + T-phase + Liqα	38.99	57.80	3.21
MWE 37B				$MgCl_2 \cdot 6H_2O$ + T-phase + Liqα	39.08	58.38	2.54
MWE 39A	39.50	54.50	6.00	$MgCl_2 \cdot 6H_2O$ + T-phase + Liqα	38.87	56.67	4.46
MWE 41A	13.50	1.50	85.00	T-phase + $MgCl_2 \cdot 3EG$ + Liqβ	14.26	1.90	83.84
MWE 41B				T-phase + $MgCl_2 \cdot 3EG$ + Liqβ	14.46	1.95	83.59
MWE 43A	10.32	0.97	88.71	T-phase + $MgCl_2 \cdot 3EG$ + Liqβ	12.53	1.61	85.86
MWE 44A	10.98	0.55	88.47	T-phase + $MgCl_2 \cdot 3EG$ + Liqβ	12.48	1.62	85.90

[a] EG refers to ethylene glycol, $C_2H_4(OH)_2$. [b] $MgCl_2 \cdot 3EG$ refers to the magnesium chloride triglycollate phase.

These four regions have been included in Figure 4; however, their existence was not verified since reaction kinetics would be sluggish due to the absence of any liquid phase.

Effect of Temperature. Phase relations were investigated over the temperature range (293 to 363) K to examine if the position of the solid−liquid phase boundary changed significantly. Temperatures within the dehydration column were known to vary within these limits, and if conditions in the dehydration column could be controlled such that a solid precipitate was not formed, then scaling would be avoided.

Experiments used two bulk compositions equivalent to those at plates 4 and plate 5 of dehydration column no. 1 at AMC's Demonstration Plant. Compositions at each plate were determined using PRO/II Simulation Software with the calculated composition for plate 4: 18.21 % $MgCl_2$, 0.49 % $CaCl_2$, 38.41 % H_2O, and 42.89 % $C_2H_4(OH)_2$, and the composition for plate 5: 13.39 % $MgCl_2$, 0.35 % $CaCl_2$, 7.67 % H_2O, and 78.94 % $C_2H_4(OH)_2$. Although the leach liquor fed to the dehydration columns contained some calcium (an impurity from the original magnesite ore), for these experiments the $CaCl_2$ was replaced

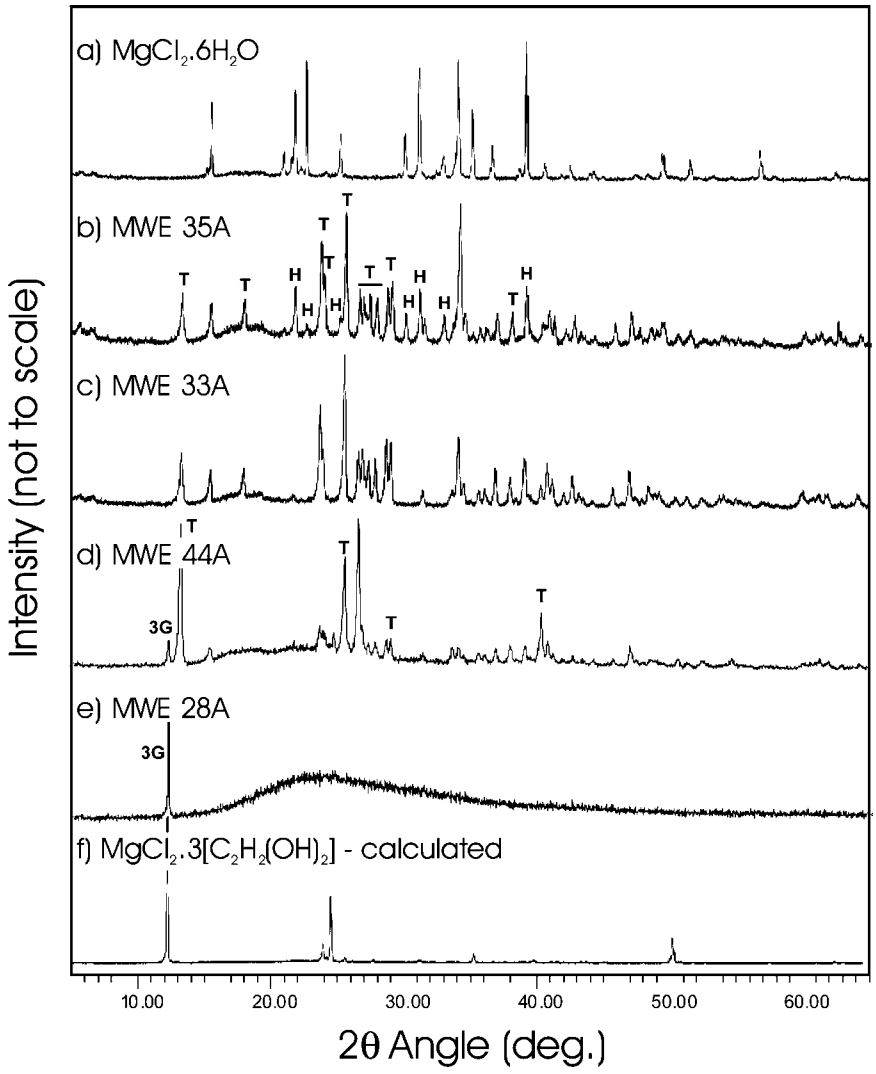

Figure 2. Representative X-ray powder diffraction patterns of solid phases: (a) $MgCl_2 \cdot 6H_2O$ starting material, (b) a mixture of $MgCl_2 \cdot 6H_2O$ and T-phase (MWE 35A), (c) T-phase (MWE 33A), (d) T-phase and magnesium chloride triglycollate (MWE 44A), and (e) magnesium chloride triglycollate (MWE 28A). Pattern (f) is the calculated pattern for magnesium chloride triglycollate. Patterns (a) to (c) were collected on samples dried at 333 K, whereas patterns (d) to (e) were X-rayed moist due to problems in drying the triglycollate phase (see text). H refers to the hexahydrate, T the T-phase, and 3G the triglycollate.

by $MgCl_2$ in the final solutions to simplify the system and to ensure that the results were compatible with the phase relations determined above.

Reaction conditions and results for tests using MWE 71 and MWE 105 are shown in Table 2. The starting bulk composition for test MWE 71 was initially plotted just within the ternary liquid-phase region. Decreasing the temperature from (353 to 294) K did not result in any precipitate forming, and the final liquid composition, after assay, was similar to the starting bulk composition as would be expected. Since no solid phase formed, the position of the solid−liquid phase boundary appears fairly insensitive to temperature changes in this region of the ternary system.

Table 2. Starting Compositions and Reaction Conditions for Tests MWE 71 and MWE 105

	bulk composition (%)			final temp.	
run no.	$MgCl_2$	H_2O	EG[a]	(K)	assemblage
MWE 71	18.70	38.40	42.90	352.4	liquid-only
				344.8	liquid-only
				331.3	liquid-only
				310.5	liquid-only
				294.0	liquid-only
MWE 105	13.39	7.67	78.94	363.4	liquid-only
				353.0	liquid-only
				343.0	liquid-only
				334.5	T-phase + liquid

[a] EG refers to ethylene glycol, $C_2H_4(OH)_2$.

For MWE 105, the original bulk composition remained a liquid at the starting temperature of 363 K, indicating it was within the ternary liquid-phase region. However, when plotted on the 333 K $MgCl_2-H_2O-C_2H_4(OH)_2$ ternary phase diagram (Figure 4), composition MWE 105 plots just within the phase field $T + Liq_T$. It was predicted therefore that, as the temperature was lowered from 363 K, a solid phase would precipitate somewhere close to, but slightly above, 333 K. A solid was precipitated when the reaction vessel was cooled to 334.5 K, which when assayed for Mg and H_2O, gave a composition containing 36.7 % $MgCl_2$, 18.6 % H_2O, and 44.7 % $C_2H_4(OH)_2$. This was very close to the ideal composition for the T-phase. X-ray diffraction analysis of the solid precipitate confirmed it to be T-phase, while assays from the separated liquid phase plot almost exactly on the solid−liquid phase boundary previously determined at 333 K.

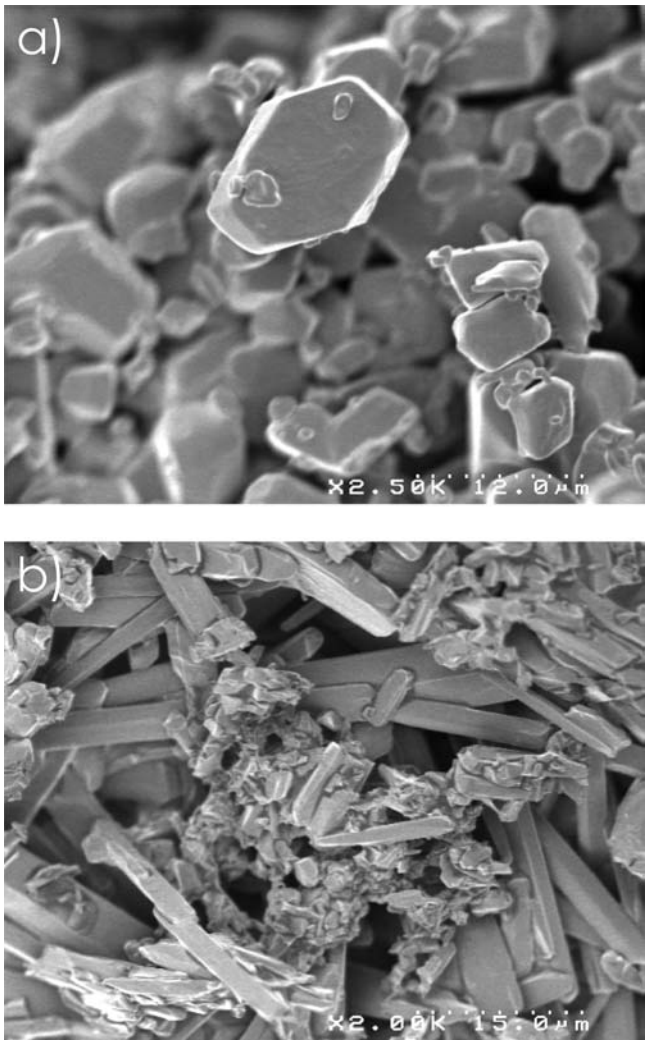

Figure 3. SEM images showing the two different crystal morphologies exhibited by the T-phase. Image (a) is from sample MWE 33, while image (b) is from sample MWE 43. Both samples were dried at 333 K.

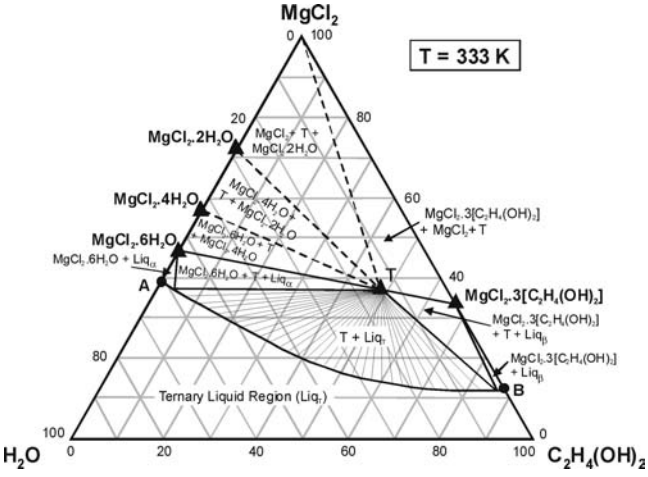

Figure 4. Interpretation of phase relations in the $MgCl_2-H_2O-C_2H_4(OH)_2$ system at 333 K. Solid triangles indicate solid phases; circles show liquid compositions along the binaries. Dashed lines indicate probable (but not experimentally verified) phase boundaries.

Results from the temperature study are illustrated qualitatively by using known solubility data along the respective binaries and constructing the solid−liquid boundary to fit the experimental observations. For example, the $MgCl_2$ solubility in H_2O decreases from 41 % (by weight) at 363 K to only 35.3 % (by weight) at 293 K.[3] Balarew et al.[7] give the solubility of $MgCl_2$ at (343 and 323) K as 39.2 % (by weight) and 37.1 % (by weight), respectively. Similarly, the solubility of $MgCl_2$ in ethylene glycol decreased from 15 % (by weight) at 363 K to 9.6 % (by weight) at 293 K (CSIRO Process Science and Engineering, unpublished work). These solubilities, along the respective binary joins and the information from runs MWE 71 and MWE 105, show the predicted change in position of the solid−liquid phase boundary with temperature in Figure 5.

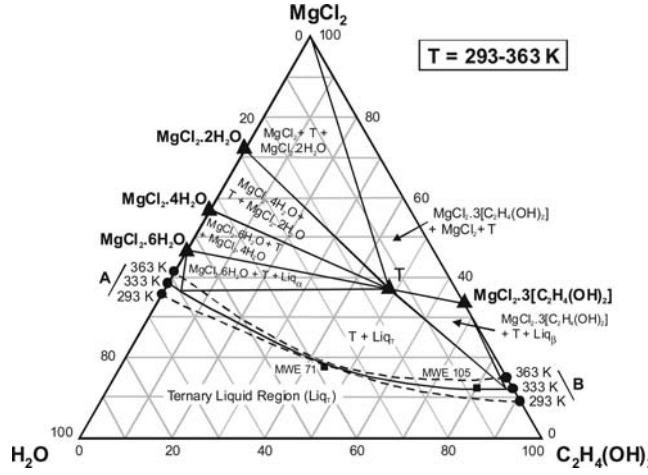

Figure 5. Phase relations in the $MgCl_2-H_2O-C_2H_4(OH)_2$ system between (293 and 363) K. Dashed lines indicate the change in location of the solid−liquid phase boundary with temperature. Solid triangles indicate solid phases; squares indicate bulk compositions MWE 71 and MWE 105. Circles show liquid compositions along the binaries at (363, 333, and 293) K.

Implications for Column Scaling. The results of the current study indicate that precipitation of the previously unknown ternary phase $MgCl_2 \cdot 2H_2O \cdot 2[C_2H_4(OH)_2]$ (T-phase) was most likely responsible for scale formation in AMC's dehydration column.

Top-feeding of the column resulted in all components of the solution passing down through the packing with the more volatile water progressively being removed from the system. As a consequence, the T-phase was precipitated when the liquid reached a critical composition within the $MgCl_2-H_2O-C_2H_4(OH)_2$ ternary. On the basis of the composition of the liquor which was fed into the dehydration column, the critical composition occurred once a temperature of around 333 K was reached. The formation of scale (T-phase) was therefore unavoidable under the operating conditions employed.

However, AMC showed that successful top-feeding of the dehydration column could be achieved through slight changes in the operating procedures. This was because an additional scale was also observed to form at the top of the column where the leach liquor was introduced. Analysis of the material by AMC indicated the presence of $Mg(OH)_2$ and Mg-oxychlorides. To counteract this additional scale, the filtered leach liquor was acidified to pH = 3.5 to 4.0 to convert soluble MgO, which could cause Mg-oxychloride at the top of the column, to $MgCl_2$. In addition, the amount of ammonia present in the dehydration column distillate was also reduced. The ammonia was contained in the recycled glycol from the crystallizer (Figure 1). Excessive ammonia led to $Mg(OH)_2$ formation at the top of the column.

Inspection of the column after the incorporation of these changed operating procedures showed that these changes also had a significant impact on the stability of the T-phase, with the packing remaining free of scale. This suggested that either

the T-phase was no longer stable under the slightly acidic operating conditions or there had been a significant change in the physical state of the T-phase. For example, the changed conditions may have resulted in the T-phase forming a smaller crystal size enabling it to flow through the packing or it may have a decreased tendency to form a wax-like, paste material.

A further point not addressed during the current study is the potential effect of reduced pressure on the stability of phases in the $MgCl_2-H_2O-C_2H_4(OH)_2$ system. The results presented above are strictly only applicable to conditions at ~1 atm total pressure. It is unknown how the phase relations translate to −90 kPa, the normal operating conditions for the dehydration column. Further work is required to examine the effect of lower pressures on scale stability.

Conclusions

Solid−liquid solubility and phase relation studies within the $MgCl_2-H_2O-C_2H_4(OH)_2$ ternary system at 333 K showed that six separate phase fields involving a liquid phase were present. These were: (1) a liquid-only phase region (Liq_T), containing $MgCl_2$, H_2O, and ethylene glycol components in solution, (2) a two-phase region T + Liq_T, (3) the two-phase regions $MgCl_2 \cdot 6H_2O$ + Liqα and $MgCl_2 \cdot 3[C_2H_4(OH)_2]$ + Liqβ, and (4) two three-phase regions characterized by the assemblages $MgCl_2 \cdot 6H_2O$ + T + Liqα and $MgCl_2 \cdot 3[C_2H_4(OH)_2]$ + T + Liqβ.

The compositions Liqα and Liqβ represent liquid compositions extending a small distance into the ternary from the invariant points A and B located along the respective $MgCl_2-H_2O$ and $MgCl_2-C_2H_4(OH)_2$ binaries, while T represents a ternary phase of composition $MgCl_2 \cdot 2H_2O \cdot 2[C_2H_4(OH)_2]$.

The solid-only phase fields $MgCl_2 \cdot 2H_2O$ + T + $MgCl_2$, $MgCl_2 \cdot 6H_2O$ + T + $MgCl_2 \cdot 4H_2O$, $MgCl_2 \cdot 4H_2O$ + T + $MgCl_2 \cdot 2H_2O$, and $MgCl_2$ + T + $MgCl_2 \cdot 3[C_2H_4(OH)_2]$ are also likely present in the system but were not confirmed in the present study.

The solid phase most likely to precipitate within the packing of the dehydration column was the ternary phase $MgCl_2 \cdot 2H_2O \cdot 2[C_2H_4(OH)_2]$.

Results of additional testwork from (293 to 363) K suggest that the position of the solid−liquid boundary does not change significantly with temperature.

Acknowledgment

The authors wish to thank Australian Magnesium Corporation (AMC) Pty. Ltd. and, in particular, Dr. Malcolm Frost and Dr. Michael Klose for valuable discussions. We also acknowledge the assistance received by Dr. Raj Rajakumar (CSIRO Light Metals Flagship) and the CSIRO Process Science and Engineering Analytical Services group for the chloride analyses. The critical reviews of two anonymous reviewers also improved the interpretation of the phase relations.

Literature Cited

(1) Jenkins, D. H.; Sheehan, G. J.; Frost, M. F. Piloting the Australian Magnesium Process. *Trans IMM Sect. C* **2009**, *118* (4), 205–213.
(2) Fanghanel, Th.; Kravchuk, K.; Voigt, W.; Emons, H.-H. The binary system $MgCl_2$-H_2O at 130−250°C. *Z. Anorg. Allg. Chem.* **1987**, *547*, 21–26.
(3) Linke, W. F. Solubilities - Inorganic and metal-organic compounds. *Am. Chem. Soc.* **1965**, *2*, 480.
(4) Braithwaite, D. D.; Allain, R. J. Anhydrous magnesium chloride using ethylene glycol and ammonia. US Patent 3,966,888, 1976.
(5) Allain, R. J. A new economical process for making anhydrous magnesium chloride. In *Light Metals 1980*; McMinn, C. J., Ed.; AIME: Warrendale, PA, 1980; pp 929−936.
(6) Sheehan, G. J.; Wong, F. S.; Hourn, M. M.; Kodama, M.; Jenkins, D. H. Anhydrous magnesium chloride. US Patent 6,143,270, 2000.
(7) Balarew, Chr.; Tepavitcharova, S.; Rabadjieva, D.; Voigt, W. Solubility and crystallization in the system $MgCl_2$-$MgSO_4$-H_2O at 50 and 75°C. *J. Solution Chem.* **2001**, *30* (9), 815–823.

Received for review March 25, 2010. Accepted June 4, 2010.

JE100293K